Diversity mediates land-surface phenology in Zambian deciduous woodlands

John L. Godlee

26th July 2021

Abstract

Land-surface phenology is a key determinant of ecosystem function across the dry tropics, and measures of land-surface phenology are routinely included in earth system models to constrain estimates of productivity. Future variation in phenology can be predicted to some extent from climatic variables, but our understanding of how ecosystem structure and composition mediates variation in phenology is lacking, commonly limited to coarse plant functional types. We combined a dense plot network of 617 sites across deciduous Zambian woodlands with remotely sensed land-surface phenology metrics to investigate the role of tree species diversity, composition, and tree size on phenological patterns, including the phenomenon of pre-rain green-up. We found that tree species diversity caused earlier pre-rain green-up across all studied vegetation types, and caused longer season length in drier woodlands. We found variation among miombo and non-miombo vegetation types in their phenological patterns and biotic drivers of phenology. Finally, we found that species evenness had contrasting effects on phenology to species diversity, suggesting that land-surface phenology is driven by a few dominant canopy-forming tree species in dry tropical woodlands. The study clarifies the role of biotic diversity as a determinant of ecosystem function, and offers new insights into the factors which determine land-surface phenology across the dry tropics, which are essential for earth system modelling approaches.

Introduction

The seasonal timing and duration of foliage production (land-surface phenology) is a key mediator of land-atmosphere exchanges. Foliage forms the primary interface between plants, the atmosphere and sunlight (Gu et al., 2003; Penuelas et al., 2009), and land-surface phenology plays an important role in regulating global carbon, water and nitrogen cycles (Richardson et al., 2013). Carbon-cycling models routinely incorporate land-surface phenological processes, most commonly through remotely-sensed data products (e.g. Bloom et al. 2016), but our understanding of the ecological mechanisms which determine these phenological processes remains under-developed (Whitley et al., 2017). This limits our ability to predict how land-surface phenology will respond to climate and biodiversity change, and how these responses will vary among species and vegetation types (Xia et al., 2015).

At regional scales, land-surface phenology can be predicted using only climatic factors, namely precipitation, diurnal temperature, and light environment (Adole et al., 2018b), but significant local variation exists within biomes in the timing of leaf production which cannot be attributed solely to abiotic environment (Stöckli et al., 2011). It has been repeatedly suggested that the diversity, composition, and demographic structure of plant species plays a role in determining how ecosystems respond to abiotic cues that may drive phenology (Adole et al., 2018a; Jeganathan et al., 2014; Fuller, 1999), owing to differences in life history strategy among species and demographic groups, but current implementation of biotic variation in earth system models is often limited to coarse plant functional types, which are unable to represent the wide variation in phenological patterns observed at local scales (Scheiter et al., 2013; Pavlick et al., 2013).

Across the dry tropics, seasonal oscillations in water availability produce strong cycles of foliage production (Chidumayo, 2001; Dahlin et al., 2016), with knock-on effects for ecosystem function. The phenomenon of pre-rain green-up seen in some tree species within the dry tropics serves as a striking example of adaptation to seasonal variation in water availability (Ryan et al., 2017). Conservative species, i.e. slower growing, with robust leaves and denser wood, may initiate leaf production (green-up) before the wet season has commenced. More acquisitive species and juveniles however, tend to green-up during the wet season creating a dense leaf-flush during the mid-season peak of growth and dropping their leaves earlier as the wet season ends (Lasky et al., 2016). Both strategies have associated costs and benefits which allow coexistence of species exhibiting a range of phenological syndromes along this spectrum. While conservative species gain a competitive advantage from having fully emerged leaves when the wet season starts, they must also invest heavily in deep root architecture to access dry season groundwater reserves in order to produce foliage during the dry season. Similarly, while acquisitive species minimise the risk of hydraulic failure and mortality by only producing leaves when conditions are amenable, they forfeit growing season length. It has been suggested that variation in phenological strategy among tree species is one mechanism by which increased species diversity increases resilience to drought and maximises productivity in water-limited woodland ecosystems (Stan & Sanchez-Azofeifa, 2019; Morellato et al., 2016). By providing functional redundancy within the ecosystem, leaf production can be maintained under a wider range of conditions, therefore maximising long-term productivity.

In addition to determining productivity, variation in leaf phenology also affects broader ecosystem function. Woodlands with a longer tree growth period support a greater diversity and abundance of wildlife, particularly birds, but also browsing mammals and invertebrates (Cole et al., 2015; Araujo et al., 2017; Morellato et al., 2016; Ogutu et al., 2013). As climate change increases the frequency and severity of drought in water-limited woodlands, it is feared that this will result in severe negative consequences for biodiversity (Bale et al., 2002). The periods of green-up and senescence which bookend the growing season are key times for invertebrate reproduction (Prather et al., 2012) and herbivore browsing activity (Velasque & Del-Claro, 2016; Morellato et al., 2016). Pre-rain green-up provides a valuable source of moisture and nutrients before the wet season, and can moderate the understorey microclimate, increasing humidity, reducing UV exposure, moderating diurnal oscillations in temperature, and reducing ecophysiological stress which otherwise can lead to mortality during the dry season. Additionally, a slower rate of green-up caused by tree species

greening at different times, i.e. reduced synchronicity, provides an extended period of bud-burst, maintaining the important food source of nutrient rich young leaves for longer. Thus, understanding the determinants of seasonal patterns of tree leaf production in dry deciduous woodlands can provide valuable information on spatial variation in their vulnerability to climate change, and help to model the contribution of these woodlands to earth system fluxes under climate change.

In this study we investigated how tree species diversity, composition, and demographic structure influence three key measurable aspects of the tree phenological cycle of dry tropical woodlands: (1) the lag time between green-up/senescence and the start/end of the wet season, (2) the rates of greening and senescence at the start and end of the seasonal growth phase, and (3) the overall length of the growing period. We hypothesise that: (H_1) sites with greater species diversity will exhibit a longer growing season and greater cumulative green-ness over the course of the growing season, due to a higher diversity of phenological strategies. Additionally, we hypothesise that: (H_2) in sites with greater species diversity the start of the growing season will occur earlier with respect to the onset of rain due to an increased likelihood of containing a species which can green-up early, and that (H_3) due to variation among species in phenological strategy and minimum water requirement, sites with greater tree species diversity will exhibit slower rates of greening and senescence as different species green-up and senesce at different times. We further hypothesise that: (H_4) irrespective of species diversity, variation in tree species composition and vegetation type will cause variation in the phenological metrics outlined above. Finally, we hypothesise that: (H_5) sites with larger trees will exhibit earlier pre-rain green-up and later senescence, under the assumption that large trees can better access resilient deep groundwater reserves outside of the wet season.

Materials and methods

Plot data

We used data on tree species diversity and composition across 617 sites from the Zambian Integrated Land Use Assessment Phase II (ILUA-II), conducted in 2014 (Mukosha & Siampale, 2009; Pelletier et al., 2018). Each site consisted of four 20x50 m (0.1 ha) plots positioned in a square around a central point, with a distance of 500 m between each plot (Figure 2). The original census contained 993 sites, which was filtered in order to define study bounds and to ensure data quality. Only sites with $\geq$50 stems ha^{-1} $\geq$10 cm DBH (Diameter at Breast Height) were included in the analysis, to ensure all sites represented woodlands rather than 'grassy savanna', which is considered a separate biome with different species composition and ecosystem processes governing phenology (Parr et al., 2014). Sites dominated by non-native tree species ($\geq$50% of individuals), e.g. *Pinus* spp. and *Eucalyptus* spp. were excluded, as these species may exhibit atypical patterns of foliage production (Broadhead et al., 2003). Of the 56634 trees recorded, 90.3% were identified to species, 1.9% were identified to genus only, 0.1% were identified to family only, and 7.7% could not be identified at all. There were no significant correlations between the number of trees identified per site and any of the phenological metrics, diversity or structural variables used in analyses.

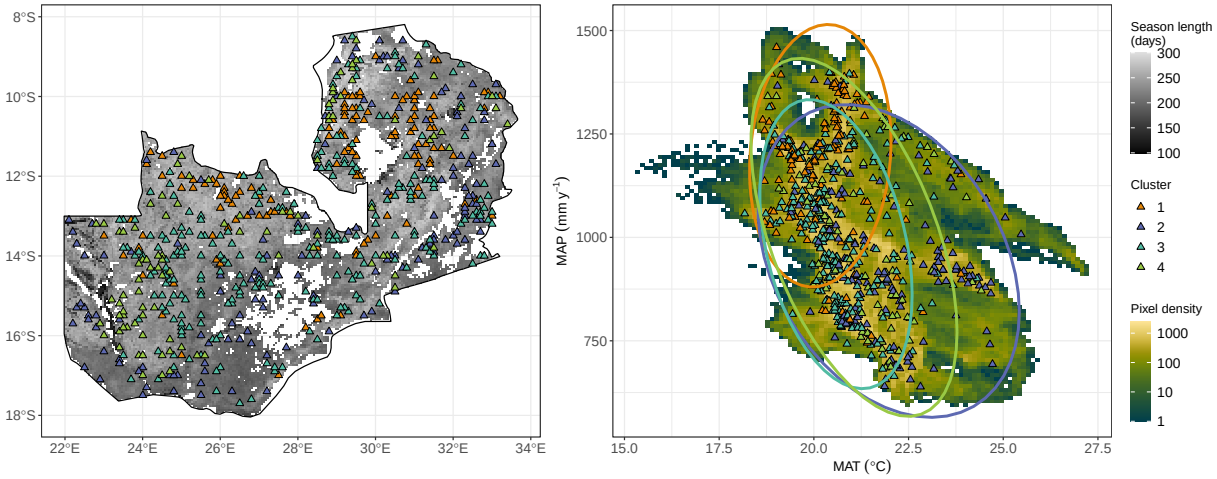

Figure 1: Distribution of study sites, within Zambia (left), and in climate space (right). Sites are shown as triangles, each consisting of four plots, coloured according to vegetation type cluster. Zambia is shaded according to growing season length, estimated by the MODIS VIPPHEN-EVI2 product, at 0.05° spatial resolution (Didan & Barreto, 2016). The growing season length layer is masked by the MODIS MCD12Q1 land cover map from 2015 (Friedl & Sulla-Menashe, 2019), using the International Geosphere-Biosphere Programme (IGBP) classification to remove all pixels occurring in wetlands, croplands, water bodies, and urban areas. Climate space is represented by Mean Annual Temperature (MAT) and Mean Annual Precipitation (MAP), extracted from the WorldClim dataset at 30 arc second resolution, between 1970 and 2000 (Fick & Hijmans, 2017). The shaded area in the right panel shows the climate space of Zambia, showing the density of pixels for given values of MAT and MAP. The ellipses in the right panel show the 95% confidence interval for the climate space of each site.

Cluster	N sites	Richness	MAP	δT	Species	Indicator value
1	134	17(7)	1176(156.1)	13(1.5)	*Brachystegia longifolia*	0.397
					Uapaca kirkiana	0.390
					Marquesia macroura	0.285
2	144	14(5)	955(172.8)	14(1.6)	*Combretum molle*	0.258
					Lannea discolor	0.228
					Combretum zeyheri	0.214
3	243	17(6)	997(157.8)	14(1.5)	*Julbernardia paniculata*	0.559
					Brachystegia boehmii	0.540
					Pseudolachnostylis maprouneifolia	0.226
4	96	14(6)	1012(185.5)	14(1.7)	*Brachystegia spiciformis*	0.582
					Cryptosepalum exfoliatum	0.285
					Guibourtia coleosperma	0.281

Table 1: Climatic information and Dufrene-Legendre indicator species analysis for the vegetation type clusters identified by the PAM algorithm, based on basal area weighted species abundances. The three species per cluster with the highest indicator values are shown along with other key statistics for each cluster. MAP (Mean Annual Precipitation) and δT (Diurnal temperature range) are reported as the mean and 1 standard deviation in parentheses. Species richness is reported as the median and the interquartile range in parentheses.

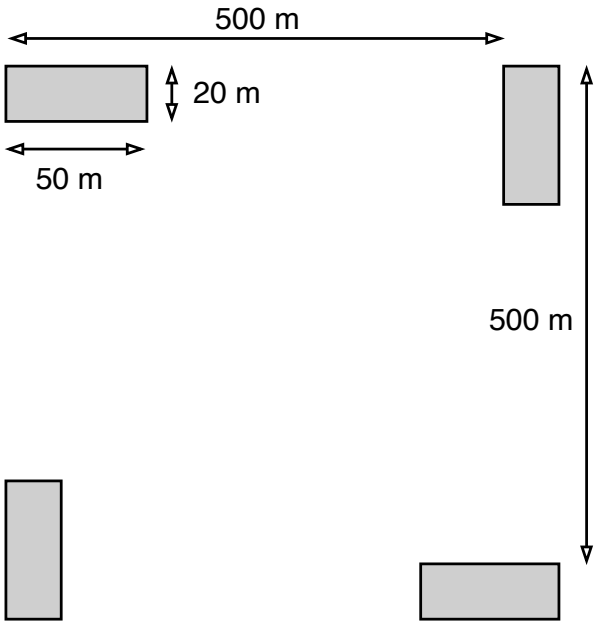

Figure 2: Schematic diagram of plot layout within a site. Each 20x50 m (0.1 ha) plot is shaded grey. Note that the plot dimensions are not to scale.

Within each plot, the species of all trees with at least one stem ≥10 cm DBH were recorded. Plot data were aggregated to the site level for analyses to avoid pseudo-replication, and to link with the more spatially coarse phenology data. Tree species composition varied little among the four plots within a site, and were treated as representative of the woodland in the local area. Using the Bray-Curtis dissimilarity index on species basal area data (Faith et al., 1987), we calculated that the mean pairwise compositional distance between plots within a site was lower than the mean compositional distance across all pairs of plots in 92% of cases.

Plot data analysis

To classify variation in tree species composition we used agglomerative hierarchical clustering on species basal area data (Kreft & Jetz, 2010; Fayolle et al., 2014). To guard against sensitivity to rare individuals, which can preclude meaningful cluster delineation across such a large species compositional range, we excluded species with less than five records. We used Ward's algorithm to define clusters (Murtagh & Legendre, 2014), based on the Bray-Curtis distance between pairs of sites. We determined the optimal number of clusters by maximising the mean silhouette width among clusters (Rousseeuw, 1987). Vegetation type clusters were used later as interaction terms in linear models. We described the vegetation types represented by each of the clusters using a Dufrêne-Legendre indicator species analysis (Dufrêne & Legendre, 1997). Four vegetation type clusters were identified during hierarchical clustering. The silhouette value of the clustering algorithm reached 0.59.

To describe the species diversity of each site, we calculated the Shannon-Wiener index (H') from species basal area rather than individual abundance, as a measure of species diversity effectively weighted by a species' contribution to canopy occupancy and thus by contribution to the phenological signal. H' was transformed to the first order numbers-equivalent (^1D) of H', calculated as $e^{H'}$ (Jost, 2007). We use ^1D as the primary measure of species diversity in our statistical models, and is subsequently referred to as species diversity. Additionally, we calculated a separate measure of abundance evenness, using the Shannon Equitability index ($E_{H'}$) (Smith & Wilson, 1996). $E_{H'}$ was calculated as the ratio of basal area Shannon-Wiener diversity index to the natural log of total basal area per site. To describe average tree size, we calculated the quadratic mean of stem diameters per site (Curtis & Marshall, 2000). The quadratic mean gives more weight to large trees and is thus more

appropriate for our use, where we are interested in the contribution of large trees to land-surface phenology.

Land-surface phenology data

To quantify phenology at each site, we used the MODIS MOD13Q1 satellite data product at 250 m resolution (Didan, 2015). The MOD13Q1 product provides an Enhanced Vegetation Index (EVI) time series at 16 day intervals. EVI is widely used as a measure of vegetation growth and the cumulative sum of EVI is well-correlated with Gross Primary Productivity (GPP), thus providing a measure of land-surface phenology that is relevant to carbon cycling (Sjöström et al., 2011). We used all scenes from January 2010 to December 2020 with less than 20% cloud cover covering the study area. All sites were determined to have a single annual growing season according to the MODIS VIPPHEN product (Didan & Barreto, 2016), which assigns pixels (0.05°, 5.55 km at equator) up to three growing seasons per year. We stacked yearly data between 2010 and 2020 and fit a General Additive Model (GAM) to produce an average EVI curve (Figure 3). We estimated the start and end of the growing season using first derivatives of the GAM. The start of the growing season was identified as the first day where the model slope exceeds half of the maximum positive model slope for a continuous period of 20 or more days, using only backwards looking data, following White et al. (2009). Similarly, we defined the end of the growing season as the final day of the latest 20 day period where the GAM slope meets or exceeds half of the maximum negative slope. We estimated the length of the growing season as the number of days between the start and end of the growing season. We calculated cumulative EVI as the area under the EVI curve during the growing season, and is reported in the results divided by 1e+05, to put it on a similar scale to other variables. We estimated the green-up rate as the slope of a linear model across EVI values between the start of the growing season and the point at which the slope reduces below half of the maximum positive slope. Similarly the senescence rate was estimated as the slope of a linear model between the latest point where the slope of decrease fell below half of the maximum negative slope and the end of the growing season. We validated our calculations of cumulative EVI, mean annual EVI, growing season length, season start date, season end date, green-up rate and senescence rate with calculations made by the MODIS VIPPHEN product with linear models comparing the two datasets across our study sites (Figure 0.S1, Table 0.S1). We chose not to use the MODIS VIPPHEN product directly due to its more coarse spatial resolution (0.05°, 5.55 km at equator).

Precipitation data were gathered using the "GPM IMERG Final Precipitation L3 1 day V06" dataset, which has a pixel size of 0.1°(11.1 km at the equator) (Huffman et al., 2015), between 2010 and 2020. Daily total precipitation was separated into three periods: precipitation during the growing season (wet season precipitation), precipitation in the 90 day period before the onset of the growing season (pre-green-up precipitation), and precipitation in 90 day period before the onset of senescence at the end of the growing season (pre-senescence precipitation). Wet season limits were defined as for the EVI data, using the first derivative of a GAM to create a curve for each site using stacked yearly precipitation data, from which we estimated the half-maximum positive and negative slope to identify where the GAM model exceeded these slope thresholds for a consistent period of 20 days or more. Mean diurnal temperature range (Diurnal δT) was calculated as the mean of monthly temperature range from the WorldClim database, using the BioClim variables, with a pixel size of 30 arc seconds (926 m at the equator) (Fick & Hijmans, 2017), averaged across all years of available data (1970-2000).

We calculated the lag between the onset of the growing season and the onset of the wet season as the difference between these two dates. We performed a similar calculation to estimate the lag between the end of the growing season and the end of the wet season. These two metrics are referred to as "green-up lag" and "senescence lag" hereafter. To aid interpretation, we reversed the sign of the green-up lag measurements, so that larger values indicate earlier pre-rain green-up.

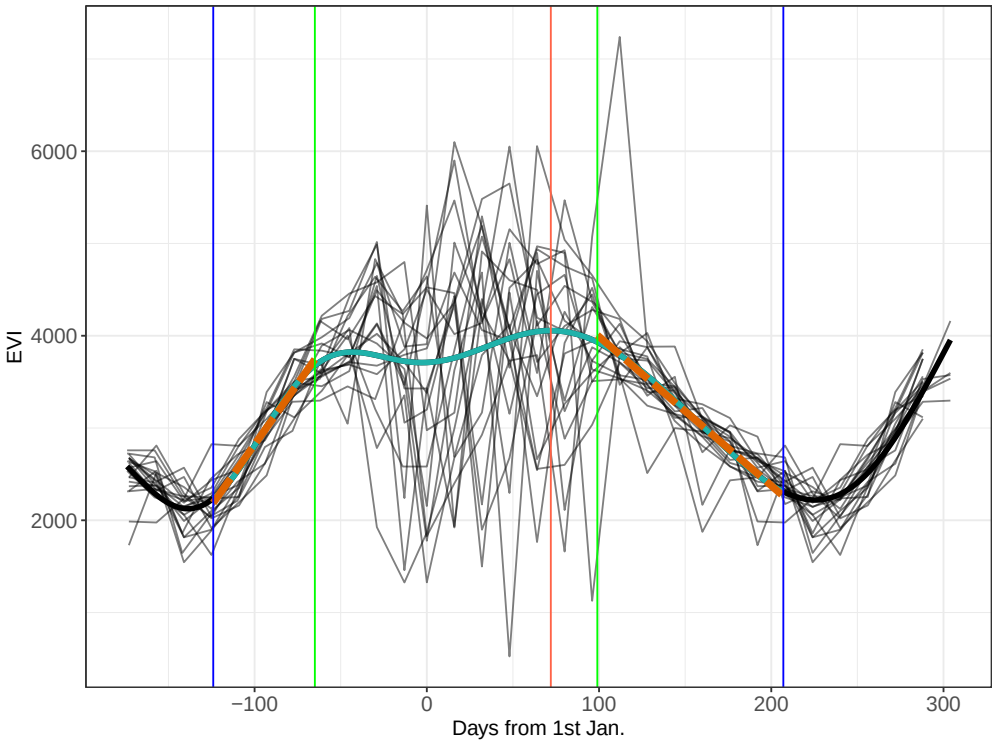

Figure 3: Example EVI time series, demonstrating the metrics derived from it. Thin black lines show the raw EVI time series, with one line for each annual growing season. The thick cyan line shows the GAM fit. The blue vertical lines show the minima which bound the growing season. The green vertical lines show the end of the green-up period and start of the senescence period, respectively. The red vertical line shows the maximum EVI value reached within the growing season. The shaded cyan area of the GAM fit shows the growing season, as defined by the first derivative of the GAM curve. The two orange dashed lines are linear regressions predicting the green-up rate and senescence rate at the start and end of the growing season, respectively. Note that while the raw EVI time series fluctuate greatly around the middle of the growing season, mostly due to cloud cover, the GAM fit effectively smooths this variation to estimate the average EVI over the 10 years of data.

Statistical modelling

We used multivariate linear models to assess the role of tree species diversity and woodland structure on each phenological metric. We defined a maximal model structure including the explanatory variables of species diversity, evenness, and tree size alongside climatic variables shown by previous studies to strongly influence land-surface phenology. We included interaction terms of species diversity, species evenness, and tree size with vegetation type. The maximal model was compared to models with different subsets of explanatory variables, using the model log likelihood, AIC (Akaike Information Criteria), and adjusted R^2 values for each model, to determine which combination of explanatory variables and their interactions with vegetation type best explained each phenological metric. Where two similar models were within 2 AIC points of each other, the model with fewer terms was chosen as the best model, to maximise model parsimony. Explanatory variables in each model were transformed to achieve normality where necessary and standardised to Z-scores prior to modelling to allow comparison of slope coefficients within a given model.

We used the `ggeffects` package to estimate the marginal means of the effects of species diversity, species evenness, and tree size on each phenological metric among vegetation types, where those terms appeared in the best model identifed durin model selection (Lüdecke, 2018). Estimating marginal means entails generating model predictions across values of a focal variable, while holding non-focal variables constant at their reference value.

To describe variation in land-surface phenology within and among vegetation clusters we conducted a simple MANOVA using the phenological metrics as response variables, followed by post-hoc Tukey's tests between each pairwise combination of vegetation clusters per phenological metric, to test whether vegetation clusters differed significantly in their land-surface phenology. We also visually compared the mean EVI GAM fits for each cluster within the growing season. All statistical analyses were conducted in R version 4.0.2 (R Core Team, 2020).

Results

Our models effectively predicted cumulative EVI, season length, green-up lag, and green-up rate, while senescence lag and senescence rate were poorly constrained even in the best fitting models. Nevertheless, all models were of better quality than a naive model including only mean annual precipitation and mean annual diurnal temperature range (Table 2). Model selection showed that both tree species diversity and evenness were significant predictors of cumulative EVI, growing season length, and green-up lag, while senescence lag, senescence rate, and green-up rate were better explained by climate only (Figure 5). Despite the 'best' model for senescence lag including diversity as an explanatory variable, the slope of this effect was negligible, with a wide standard error, and the model itself only explained 11%.

As expected (H_1), species diversity and wet season precipitation both had positive significant effects on cumulative EVI and growing season length. In contrast, abundance evenness, the other aspect of tree species diversity in our models, had a significant negative effect on these three phenological metrics (Figure 5). Similarly, species diversity increased green-up lag, i.e. the length of the period between green-up and wet season onset, while evenness caused a decrease in green-up lag (H_2). The positive effect of diversity was comparable to the effects of pre-green-up precipitation and diurnal temperature range, which also increased green-up lag. The best model predicting green-up lag explained 32% of the variance in this phenological metric.

Larger average tree size, measured by the quadratic mean of stem DBH per site, was only included and significant in the best model for senescence lag, where it caused earlier senescence with respect to the end of the wet season (H_5). None of the other phenological metrics were significantly affected by average tree size. As mentioned previously however, senescence lag was poorly constrained in our models, with the best model explaining only 11% of the variance in senescence lag.

Vegetation type clusters exhibited some spatial and climatic stratification (Figure 1). The key emergent trends were that Cluster 1 was largely absent from the southwest of the country, occurring predominantly in higher rainfall regions. Cluster 4 dominated the southwest of the country, possibly representing drier Angolan miombo woodland (Table 1). Of the four vegetation clusters identified, Cluster 2, consists of small stature Zambesian woodlands, as described by Dinerstein et al. (2017) and Chidumayo (2001), and is not dominated by the same archetypal Detarioideae canopy tree species as miombo woodland. It is possible that these woodlands represent highly disturbed miombo woodlands where large trees may have been removed by humans or by fire induced mortality. Cluster 2 occurs over a wide climatic range, and contains some of the warmest sites in the dataset. Clusters 1, 3 and 4 represent varieties of miombo woodland, dominated by *Brachystegia* spp. and *Julbernardia* spp., with different secondary species. Median species richness and the range of species richness values per site is similar across vegetation clusters (Table 1).

The slope of the relationship between species diversity and phenological metrics varied among vegetation types (H_4) (Figure 6). According to post-hoc Tukey's tests on marginal effects (Table 0.S8), Cluster 2 differed from all other clusters in the effect of species diversity on cumulative EVI, growing season length, and pre-rain green-up lag. Clusters 1 and 4 appear to show no positive effect of diversity on cumulative EVI and Cluster 4 also showed a negative effect of diversity on season length. The effect of diversity and evenness on green-up lag were consistent among all vegetation types. Cluster 2 appears to show a divergent positive effect of evenness on cumulative EVI compared to the other clusters.

Clusters, 1, 3 and 4 were largely similar in their density distribution of the six phenological metrics, while Cluster 2 had more plots with lower cumulative EVI and a shorter growing season (Figure 7). A MANOVA including all phenological metrics showed a significant difference among vegetation clusters ($F(3,613)=14.06$, $p<0.01$). Post-hoc Tukey's tests showed significant differences between Cluster 2 and the other three clusters for all phenological metrics (Table 0.S9). Cluster 2 had a significantly shorter growing season than the other clusters, caused by both later green-up and earlier senescence. Cluster 2 also had a higher maximum EVI than the other clusters (Figure 4). The vast majority of plots, regardless of vegetation type, exhibited some degree of pre-rain green-up, and all plots exhibited some degree of senescence lag (Figure 7).

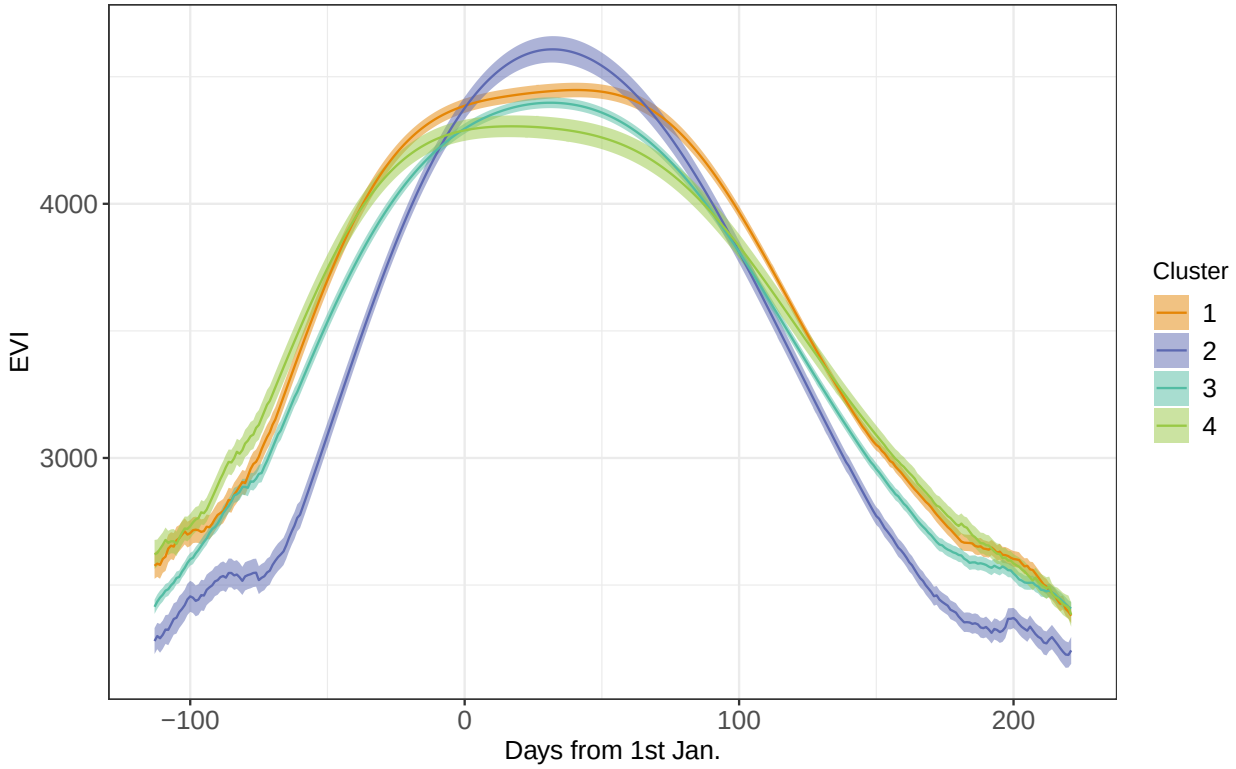

Figure 4: Mean GAMs of EVI over the growing season for each vegetation type cluster. Shaded ribbons are 95% confidence intervals.

Response	δAIC	R^2_{adj}	δlogLik
Cumulative EVI	74.8	0.34	-52.38
Season length	75.3	0.20	-52.63
Green-up rate	48.2	0.21	-39.09
Senescence rate	83.2	0.15	-56.59
Green-up lag	100.3	0.33	-65.15
Senescence lag	21.3	0.11	-25.64

Table 2: Model fit statistics for the best model describing each phenological metric.

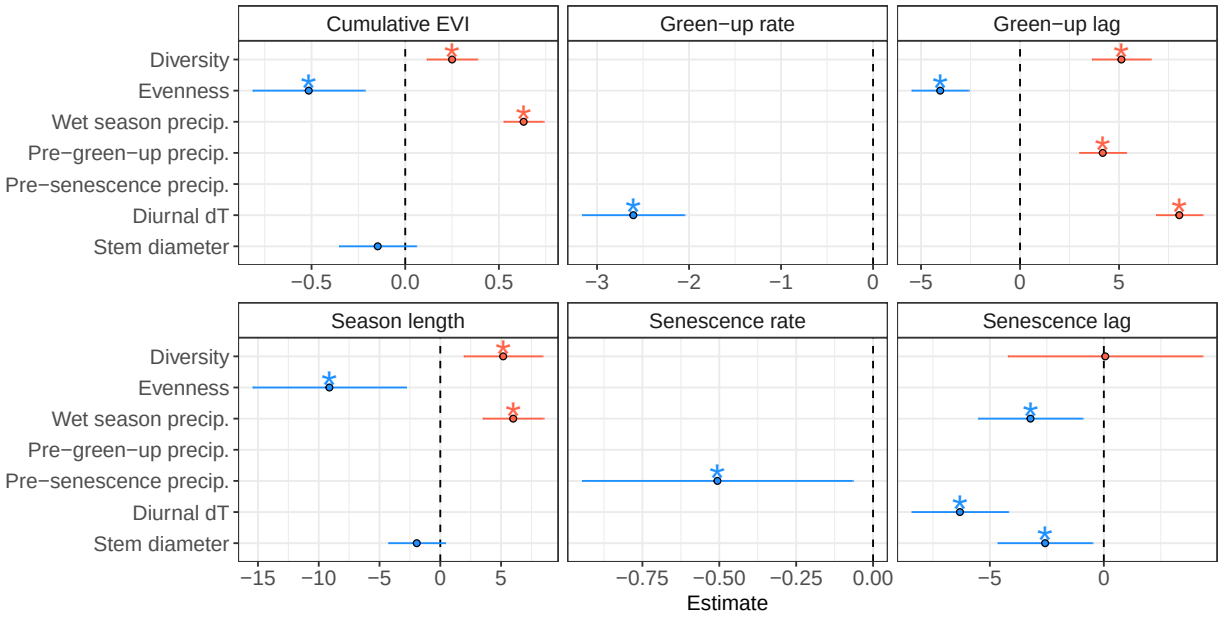

Figure 5: Standardized slope coefficients for each best model of a phenological metric. Slope estimates are ±1 standard error. Slope estimates where the interval does not overlap zero are considered to be significant effects and are marked by asterisks.

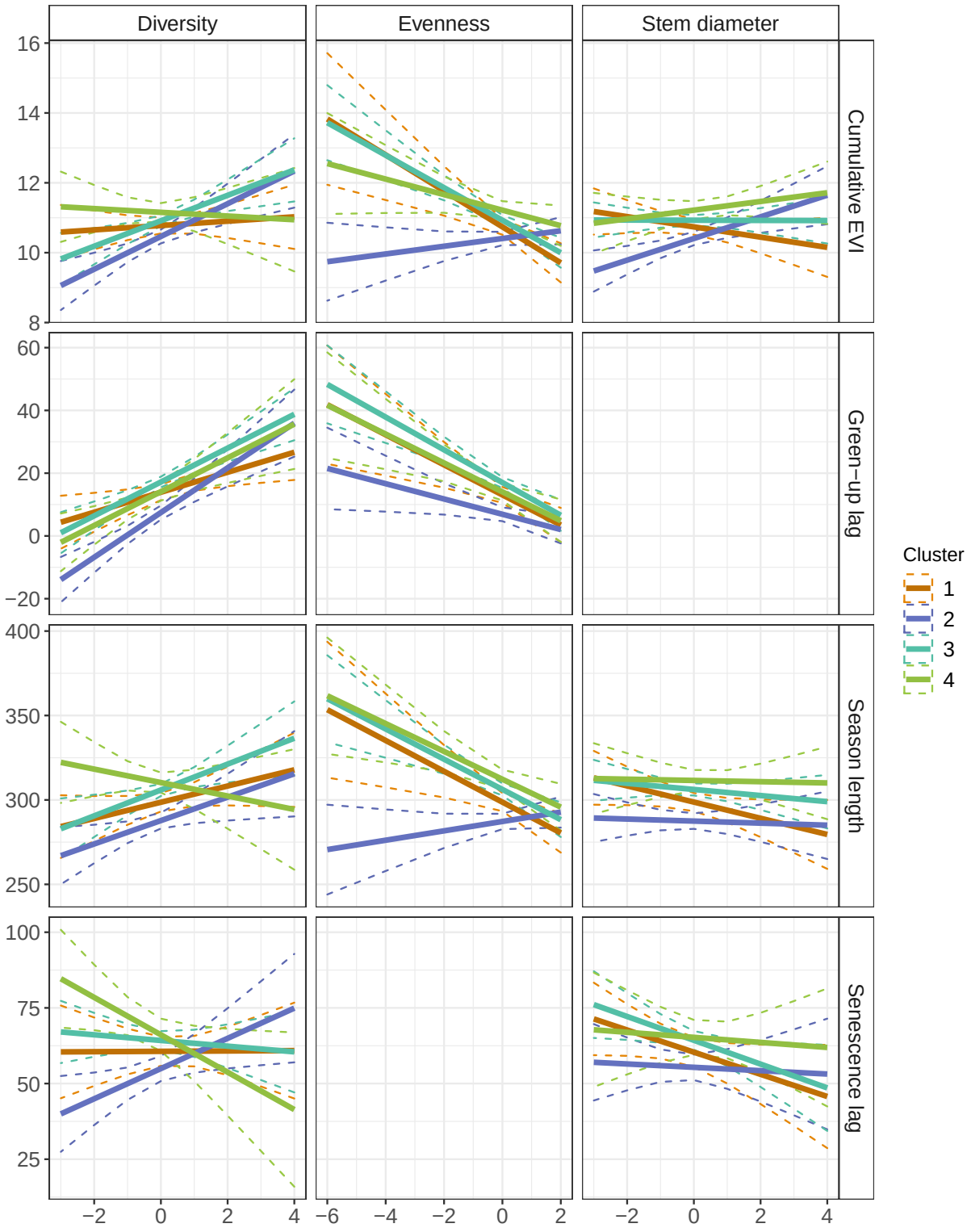

Figure 6: Marginal effects of tree species diversity, evenness, and tree size on each of the phenological metrics, using the maximal mixed effects model, for each vegetation cluster. Dotted lines represent 95% confidence intervals.

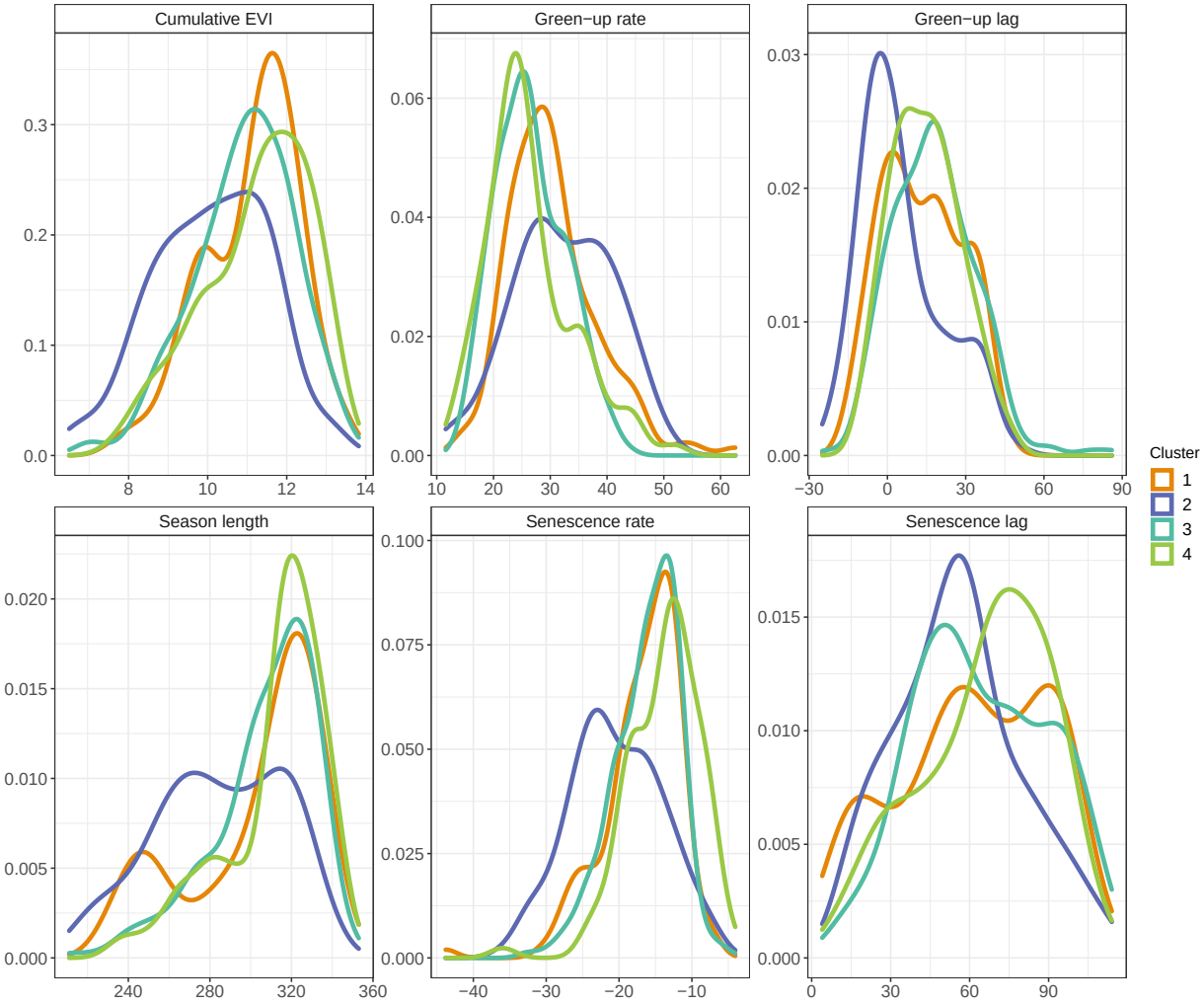

Figure 7: Density distribution of the six phenological metrics used in the study, grouped by vegetation cluster.

Discussion

In this study we have demonstrated clear and measurable effects of tree species diversity, evenness, and composition on various aspects of land-surface phenology in Zambian deciduous savannas, independent of the effects of climatic variation. We showed that tree species diversity led to an increase in cumulative EVI and growing season length in certain vegetation types. Additionally, species diversity caused the onset of greening to occur earlier with respect to the start of the wet season, in all vegetation types. Our study lends support for a positive biodiversity-ecosystem function relationship in deciduous savannas, operating through its influence on land-surface phenology, with a longer growing season and greater cumulative EVI suggesting greater primary productivity in species rich woodlands. Additionally, our finding that species diversity causes earlier pre-rain green-up suggests that diverse woodlands are more resilient to varying precipitation patterns, by producing foliage in advance of seasonal rainfall. This provides early forage for herbivores (Morellato et al., 2016), and provides facilitative effects such as cover and hydraulic lift which benefit understorey plants (Domec et al., 2010; Yu & D'Odorico, 2015). Our results highlight the role of tree species diversity as a driver of key ecosystem processes, which affect ecosystem structure, the wildlife provisioning role, and gross primary productivity.

Our finding that species diversity strongly affects patterns of land-surface phenology in deciduous Zambian woodlands provides earth surface system modellers with a means to better understand how

future changes in species diversity and composition will affect land-surface phenology and therefore the carbon cycle. Incorporating predictions of biotic change into carbon cycling models has been limited (Ahlstrom et al., 2015; Bodegom et al., 2011), owing to large uncertainties in the effects of diversity on Gross Primary Productivity (GPP). Our study provides a link by demonstrating a strong positive relationship between species diversity and cumulative EVI, which itself correlates with GPP (Sjöström et al., 2011).

While species diversity is a common measure of biodiversity, abundance evenness constitutes a second key related axis (Wilsey et al., 2005; Hillebrand et al., 2008; Jost, 2010). In this study, we found contrasting effects of diversity and evenness on cumulative EVI, growing season length and green-up lag. Evenness caused a decrease in these phenological metrics, contrary to our hypothesis. It is possible that the negative effect of abundance evenness occurred because an increase in evenness is associated with a reduction in the dominance of a few large canopy-forming tree species (e.g. *Brachystegia* spp. and *Julbernardia paniculata*). Large canopy tree species have access to groundwater for a longer part of the year, due to their deep root systems and conservative growth patterns, allowing them to green-up in advance of seasonal rains and remain resilient to mid-season fluctuations in water availability (Zhou et al., 2020). Indeed, our study found that plots with larger trees tend to senesce later with respect to the end of the wet season. We also found that while the three miombo vegetation types showed a negative effect of evenness on cumulative EVI and season length, Cluster 2, which was not dominated by miombo canopy tree species, showed a positive effect of evenness on these phenological metrics.

The effect of species diversity on cumulative EVI and growing season length was driven largely by the response of vegetation Cluster 2, which consisted of shorter stature non-miombo vegetation. Clusters 1, and 4, which consisted of miombo vegetation, exhibited negligible species diversity effects on these two phenological metrics. However, Cluster 3, the remaining miombo vegetation type also showed a positive effect of evenness on cumulative EVI. Cluster 3 had lower annual precipitation than the other two miombo clusters, with a precipitation regime closer to that of Cluster 2. In high precipitation miombo vegetation, it appears that the dominant archetypal miombo tree species can grow to large canopy forming trees, and that these individuals determine cumulative EVI as a result. Meanwhile, in the drier woodlands represented by Clusters 2 and 3, a genuine species diversity effect driven by niche complementarity exists. We suggest that in these drier woodlands, higher species diversity provides ecosystem-level resilience to drought by increasing the breadth of water use strategies.

Patterns of senescence were poorly predicted by species diversity and evenness in our models. Cho et al. (2017) found that tree cover, measured by MODIS LAI data, had a significant negative effect on senescence rates in savannas in South Africa, which have similar climatic conditions to the sites in our study. In most savannas, including sparse savannas, while the onset of the growing season is often driven by tree photosynthetic activity, which may precede the onset of precipitation, the end of the growing season is conversely driven by the understorey grass layer, which itself can be dependent on tree cover (Cho et al., 2017; Guan et al., 2014). Grass activity is more reactive to short-term changes in soil moisture than tree activity, and may oscillate within the senescence period (Archibald & Scholes, 2007). This may explain the lack of a strong precipitation signal for senescence lag and senescence rate in our models. Our finding that sites with larger trees may prolong the growing season beyond the end of the rainy season corroborates these earlier studies. As average tree stem size increases, tree cover is also likely to increase (Panzou et al., 2020), reducing the relative contribution of the understorey grass layer to land-surface phenology and producing a more consistent decline in EVI during the senescence period.

Other studies both globally and within southern African savannas have largely ignored patterns of senescence, instead focussing patterns of green-up (Gallinat et al., 2015). Most commonly, these studies simply correlate the decline of rainfall with senescence (Stevens et al., 2016; Guan et al., 2014), but our best model suggests that diurnal temperature range is a stronger determinant of the end of the growing season than precipitation. Diurnal temperature range effectively measures mean daily temperature variability. We suggest that diurnal temperature fluctuations, particularly

minimum night time temperatures, may provide cues for senescence toward the end of the wet season. In temperate ecosystems which experience autumn senescence, lower night time temperatures have been shown to increase the rate of senescence (Michelson et al., 2017; Gárate-Escamilla et al., 2020), thus leaves remain green for longer when the diurnal temperature range is smaller. Similarly, our models showed that larger diurnal temperature range caused earlier pre-rain green-up, and possibly acts as a cue to initiate the growing season as well.

Alternatively, Zani et al. (2020) suggests that in resource limited environments, senescence times may largely be set by the preceding photosynthetic activity and sink-limitations on growth. For example, limited nutrient supply may prohibit photosynthesis late in the season if the preceding photosynthetic activity has depleted that supply. Reich et al. (1992) suggested that there are many direct constraints on leaf life-span such as drought and herbivory, especially in the dry tropics, which would lead to timing of senescence being set largely by the time of bud-burst. Our study corroborates this theory, showing that precipitation across the entire wet season was a better predictor of senescence lag than pre-senescence precipitation, while pre-senescence precipitation does cause variation in the rate of senescence. However, we did not find a strong correlation between green-up lag and senescence lag (Figure 0.S2).

While leaf senescence may not be as important for the survival of browsing herbivores as the green-up period, the timing of senescence with respect to temperature and precipitation has important consequences for the savanna understorey microclimate. The longer leaf material remains in the canopy after the end of the wet season, the greater the microclimatic buffer for herbaceous understorey plants and animals, which require water and protection from high levels of insolation and dry air which can prevail rapidly after the end of the wet season (Guan et al., 2014). Our study merely demonstrates that more work needs to be done to properly characterise the drivers of senescence in this biome, which were poorly constrained in our models.

Our coverage of very short growing season lengths in Zambia was restricted, with a notable absence of available plot data in the northeast of the country around 30.5°E, 11.5°S, and 23.0°E, 15.0°S. These regions are largely seasonally water-logged floodplain and swampland, and were likely excluded by the ILUA-II assessment for this reason. This also explains their divergent phenological patterns as observed in the MODIS EVI data (Figure 1). The plot data does however, provide representative coverage of growing season lengths in wooded ecosystems. While our study focusses on woodlands, the phenological behaviour of these other vegetation types should also be considered in future studies, as these may be even more sensitive to changes in climate (Dean et al., 2018) and under greater land-use change pressures (Langan et al., 2018).

It is important to note that the remotely sensed EVI measurements used here aren't specific only to trees, they represent the landscape as a singe unit. Nevertheless, seasonal patterns of tree leaf phenology in southern African deciduous woodlands, particularly the pre-rain green-up phenomenon, is driven almost exclusively by trees, while grass phenology tends to follow patterns of precipitation more closely (Whitecross et al., 2017; Archibald & Scholes, 2007; Higgins et al., 2011). Grasses contribute to gross primary productivity, and it was therefore in our interests to include their response in our analysis as we seek to demonstrate how tree species diversity can affect cycles of carbon exchange. Additionally, the micro-climatic effects of tree leaf canopy coverage and hydraulic lift through tree deep root systems will benefit the productivity of grasses as well as understorey tree individuals.

Conclusion

Here we explored the role of tree species diversity, composition and woodland structure on land surface phenology across Zambia. We showed that species diversity clearly causes earlier pre-rain green-up, across all vegetation types studied here. The length of the growing season, and ultimately woodland productivity as measured by cumulative EVI, appeared to increase with species diversity in drier woodlands only, while wetter miombo woodlands were dominated by a few canopy-forming

archetypal miombo Detarioideae species regardless of species diversity. Interestingly, species evenness had a consistently negative effect on green-up lag, suggesting that pre-rain green-up is driven by dominant species. Finally, we have demonstrated variation in phenological patterns among vegetation types within Zambia that are commonly not distinguished in earth system models. Our results have a range of consequences for earth system modellers as well as conservation managers working in Zambia and across the dry tropics, and lend further support to an already well established corpus of the positive effect of species diversity on ecosystem function.

References

Adole, T., J. Dash & P. M. Atkinson (2018a). 'Characterising the land surface phenology of Africa using 500 m MODIS EVI'. In: *Applied Geography* 90, pp. 187–199. DOI: 10.1016/j.apgeog.2017.12.006.

— (2018b). 'Large-scale prerain vegetation green-up across Africa'. In: *Global Change Biology* 24.9, pp. 4054–4068. DOI: 10.1111/gcb.14310.

Ahlstrom, A., M. R. Raupach, G. Schurgers, B. Smith, A. Arneth, M. Jung, M. Reichstein, J. G. Canadell, P. Friedlingstein, A. K. Jain et al. (2015). 'The dominant role of semi-arid ecosystems in the trend and variability of the land CO2 sink'. In: *Science* 348.6237, pp. 895–899. DOI: 10.1126/science.aaa1668.

Araujo, H. F. P. de, A. H. Vieira-Filho, M. R. V. Barbosa, J. A. F. Diniz-Filho & J. M. C. da Silva (2017). 'Passerine phenology in the largest tropical dry forest of South America: Effects of climate and resource availability'. In: *Emu - Austral Ornithology* 117.1, pp. 78–91. DOI: 10.1080/01584197.2016.1265430.

Archibald, S. & R. J. Scholes (2007). 'Leaf green-up in a semi-arid African savanna -separating tree and grass responses to environmental cues'. In: *Journal of Vegetation Science* 18.4, pp. 583–594. DOI: 10.1111/j.1654-1103.2007.tb02572.x.

Bale, J. S., G. J. Masters, I. D. Hodkinson, C. Awmack, T. M. Bezemer, V. K. Brown, J. Butterfield, A. Buse, J. C. Coulson, J. Farrar et al. (2002). 'Herbivory in global climate change research: direct effects of rising temperature on insect herbivores'. In: *Global Change Biology* 8.1, pp. 1–16. DOI: 10.1046/j.1365-2486.2002.00451.x.

Bloom, A. A., J. Exbrayat, I. R. van der Velde, L. Feng & M. Williams (2016). 'The decadal state of the terrestrial carbon cycle: Global retrievals of terrestrial carbon allocation, pools, and residence times'. In: *Proceedings of the National Academy of Sciences* 113.5, pp. 1285–1290. DOI: 10.1073/pnas.1515160113.

Bodegom, P. M. Van, J. C. Douma, J. P. M. Witte, J. C. Ordoñez, R. P. Bartholomeus & R. Aerts (2011). 'Going beyond limitations of plant functional types when predicting global ecosystem-atmosphere fluxes: exploring the merits of traits-based approaches'. In: 21.6, pp. 625–636. DOI: 10.1111/j.1466-8238.2011.00717.x.

Broadhead, J. S., C. K. Ong & C. R. Black (2003). 'Tree phenology and water availability in semi-arid agroforestry systems'. In: *Forest Ecology and Management* 180.1-3, pp. 61–73. DOI: 10.1016/s0378-1127(02)00602-3.

Chidumayo, E. N. (2001). 'Climate and phenology of savanna vegetation in southern Africa'. In: *Journal of Vegetation Science* 12.3, p. 347. DOI: 10.2307/3236848.

Cho, M. A., A. Ramoelo & L. Dziba (2017). 'Response of land surface phenology to variation in tree cover during green-up and senescence periods in the semi-arid savanna of southern Africa'. In: *Remote Sensing* 9.7, p. 689. DOI: 10.3390/rs9070689.

Cole, E. F., P. R. Long, P. Zelazowski, M. Szulkin & B. C. Sheldon (2015). 'Predicting bird phenology from space: Satellite-derived vegetation green-up signal uncovers spatial variation in phenological synchrony between birds and their environment'. In: *Ecology and Evolution* 5.21, pp. 5057–5074. DOI: 10.1002/ece3.1745.

Curtis, Robert O. & David D. Marshall (2000). 'Technical Note: Why Quadratic Mean Diameter?' In: 15.3, pp. 137–139. DOI: 10.1093/wjaf/15.3.137.

Dahlin, Kyla M., Dominick Del Ponte, Emily Setlock & Ryan Nagelkirk (2016). 'Global patterns of drought deciduous phenology in semi-arid and savanna-type ecosystems'. In: *Ecography* 40.2, pp. 314–323. DOI: 10.1111/ecog.02443.

Dean, Joshua F., Jack J. Middelburg, Thomas Röckmann, Rien Aerts, Luke G. Blauw, Matthias Egger, Mike S. M. Jetten, Anniek E. E. de Jong, Ove H. Meisel, Olivia Rasigraf et al. (2018). 'Methane Feedbacks to the Global Climate System in a Warmer World'. In: *Reviews of Geophysics* 56.1, pp. 207–250. DOI: 10.1002/2017rg000559.

Didan, L. (2015). *MOD13Q1 MODIS/Terra Vegetation Indices 16-Day L3 Global 250m SIN Grid V006 [Data set]*. NASA EOSDIS Land Processes DAAC. DOI: 10.5067/MODIS/MOD13Q1.006. (Visited on 05/08/2020).

Didan, L. & A. Barreto (2016). *NASA MEaSUREs Vegetation Index and Phenology (VIP) Phenology EVI2 Yearly Global 0.05Deg CMG [Data set]*. NASA EOSDIS Land Processes DAAC. DOI: 10.5067/MEaSUREs/VIP/VIPPHEN_EVI2.004. (Visited on 05/08/2020).

Dinerstein, Eric, David Olson, Anup Joshi, Carly Vynne, Neil D. Burgess, Eric Wikramanayake, Nathan Hahn, Suzanne Palminteri, Prashant Hedao, Reed Noss et al. (2017). 'An Ecoregion-Based Approach to Protecting Half the Terrestrial Realm'. In: *BioScience* 67.6, pp. 534–545. DOI: 10.1093/biosci/bix014.

Domec, Jean-Christophe, John S. King, Asko Noormets, Emrys Treasure, Michael J. Gavazzi, Ge Sun & Steven G. McNulty (2010). 'Hydraulic redistribution of soil water by roots affects whole-stand evapotranspiration and net ecosystem carbon exchange'. In: 187.1, pp. 171–183. DOI: 10.1111/j.1469-8137.2010.03245.x.

Dufrêne, M. & P. Legendre (1997). 'Species assemblages and indicator species: The need for a flexible asymmetrical approach'. In: *Ecological Monographs* 67.3, pp. 345–366. DOI: 10.1890/0012-9615(1997)067[0345:saaist]2.0.co;2.

Faith, Daniel P., Peter R. Minchin & Lee Belbin (1987). 'Compositional dissimilarity as a robust measure of ecological distance'. In: *Vegetatio* 69.1-3, pp. 57–68. DOI: 10.1007/bf00038687.

Fayolle, A., M. D. Swaine, J. Bastin, N. Bourland, J. A. Comiskey, G. Dauby, J. Doucet, J. Gillet, S. Gourlet-Fleury, O. J. Hardy et al. (2014). 'Patterns of tree species composition across tropical African forests'. In: *Journal of Biogeography* 41.12, pp. 2320–2331. DOI: 10.1111/jbi.12382.

Fick, S. E. & R. J. Hijmans (2017). 'WorldClim 2: New 1-km spatial resolution climate surfaces for global land areas'. In: *International Journal of Climatology* 37.12, pp. 4302–4315. DOI: 10.1002/joc.5086.

Friedl, M. & D. Sulla-Menashe (2019). *MCD12Q1 MODIS/Terra+Aqua Land Cover Type Yearly L3 Global 500m SIN Grid V006 [Data set]*. NASA EOSDIS Land Processes DAAC. DOI: 10.5067/MODIS/MCD12Q1.006. (Visited on 23/07/2021).

Fuller, D. O. (1999). 'Canopy phenology of some mopane and miombo woodlands in eastern Zambia'. In: *Global Ecology and Biogeography* 8.3-4, pp. 199–209. DOI: 10.1046/j.1365-2699.1999.00130.x.

Gallinat, A. S., R. B. Primack & D. L. Wagner (2015). 'Autumn, the neglected season in climate change research'. In: 30.3, pp. 169–176. DOI: 10.1016/j.tree.2015.01.004.

Gárate-Escamilla, Homero, Craig C. Brelsford, Arndt Hampe, T. Matthew Robson & Marta Benito Garzón (2020). 'Greater capacity to exploit warming temperatures in northern populations of European beech is partly driven by delayed leaf senescence'. In: 284, p. 107908. DOI: 10.1016/j.agrformet.2020.107908.

Gu, L., W. M. Post, D. Baldocchi, T. A. Black, S. B. Verma, T. Vesala & S. C. Wofsy (2003). 'Phenology of vegetation photosynthesis'. In: *Phenology: An Integrative Environmental Science*. Springer Netherlands, pp. 467–485. DOI: 10.1007/978-94-007-0632-3_29.

Guan, K., E. F. Wood, D. Medvigy, J. Kimball, M. Pan, K. K. Caylor, J. Sheffield, C. Xu & M. O. Jones (2014). 'Terrestrial hydrological controls on land surface phenology of African savannas and woodlands'. In: *Journal of Geophysical Research: Biogeosciences* 119.8, pp. 1652–1669. DOI: 10.1002/2013jg002572.

Higgins, S. I., M. D. Delgado-Cartay, E. C. February & H. J. Combrink (2011). 'Is there a temporal niche separation in the leaf phenology of savanna trees and grasses?' In: *Journal of Biogeography* 38.11, pp. 2165–2175. DOI: 10.1111/j.1365-2699.2011.02549.x.

Hillebrand, H., D. M. Bennett & M. W. Cadotte (2008). 'Consequences of dominance: A review of evenness effects on local and regional ecosystem processes'. In: *Ecology* 89.6, pp. 1510–1520. DOI: 10.1890/07-1053.1.

Huffman, G. J., E. F. Stocker, D.T. Bolvin, E. J. Nelkin & Jackson Tan (2015). *GPM IMERG Final Precipitation L3 1 day 0.1 degree x 0.1 degree V06 [Data set]*. Goddard Earth Sciences Data and Information Services Center (GES DISC). DOI: 10.5067/GPM/IMERGDF/DAY/06. (Visited on 30/10/2020).

Jeganathan, C., J. Dash & P. M. Atkinson (2014). 'Remotely sensed trends in the phenology of northern high latitude terrestrial vegetation, controlling for land cover change and vegetation type'. In: *Remote Sensing of Environment* 143, pp. 154–170. DOI: 10.1016/j.rse.2013.11.020.

Jost, L. (2007). 'Partitioning diversity into independent alpha and beta components'. In: *Ecology* 88.10, pp. 2427–2439. DOI: 10.1890/06-1736.1.

— (2010). 'The relation between evenness and diversity'. In: *Diversity* 2.2, pp. 207–232. DOI: 10.3390/d2020207.

Kreft, Holger & Walter Jetz (2010). 'A framework for delineating biogeographical regions based on species distributions'. In: *Journal of Biogeography* 37.11, pp. 2029–2053. DOI: 10.1111/j.1365-2699.2010.02375.x.

Langan, Charlie, Jenny Farmer, Mike Rivington & Jo U. Smith (2018). 'Tropical wetland ecosystem service assessments in East Africa: A review of approaches and challenges'. In: 102, pp. 260–273. DOI: 10.1016/j.envsoft.2018.01.022.

Lasky, Jesse R, María Uriarte & Robert Muscarella (2016). 'Synchrony, compensatory dynamics, and the functional trait basis of phenological diversity in a tropical dry forest tree community: effects of rainfall seasonality'. In: 11.11, p. 115003. DOI: 10.1088/1748-9326/11/11/115003.

Lüdecke, D. (2018). 'ggeffects: Tidy data frames of marginal effects from regression models.' In: *Journal of Open Source Software* 3.26, p. 772. DOI: 10.21105/joss.00772.

Michelson, Ingrid H., Pär K. Ingvarsson, Kathryn M. Robinson, Erik Edlund, Maria E Eriksson, Ove Nilsson & Stefan Jansson (2017). 'Autumn senescence in aspen is not triggered by day length'. In: 162.1, pp. 123–134. DOI: 10.1111/ppl.12593.

Morellato, L. P. C., B. Alberton, S. T. Alvarado, B. Borges, E. Buisson, M. G. G. Camargo, L. F. Cancian, D. W. Carstensen, D. F. E. Escobar, P. T. P. Leite et al. (2016). 'Linking plant phenology to conservation biology'. In: *Biological Conservation* 195, pp. 60–72. DOI: 10.1016/j.biocon.2015.12.033.

Mukosha, J. & A. Siampale (2009). *Integrated land use assessment Zambia 2005–2008*. Lusaka, Zambia: Ministry of Tourism, Environment et al.

Murtagh, F. & P. Legendre (2014). 'Ward's hierarchical agglomerative clustering nethod: Which algorithms implement Ward's criterion?' In: *Journal of Classification* 31.3, pp. 274–295. DOI: 10.1007/s00357-014-9161-z.

Ogutu, J. O., H. Piepho & H. T. Dublin (2013). 'Responses of phenology, synchrony and fecundity of breeding by African ungulates to interannual variation in rainfall'. In: *Wildlife Research* 40.8, p. 698. DOI: 10.1071/wr13117.

Panzou, Grace Jopaul Loubota, Adeline Fayolle, Tommaso Jucker, Oliver L. Phillips, Stephanie Bohlman, Lindsay F. Banin, Simon L. Lewis, Kofi Affum-Baffoe, Luciana F. Alves, Cécile Antin et al. (2020). 'Pantropical variability in tree crown allometry'. In: 30.2. Ed. by Andrew Kerkhoff, pp. 459–475. DOI: 10.1111/geb.13231.

Parr, C. L., C. E. R. Lehmann, W. J. Bond, W. A. Hoffmann & A. N. Andersen (2014). 'Tropical grassy biomes: Misunderstood, neglected, and under threat'. In: *Trends in Ecology and Evolution* 29, pp. 205–213. DOI: 10.1016/j.tree.2014.02.004.

Pavlick, R., D. T. Drewry, K. Bohn, B. Reu & A. Kleidon (2013). 'The Jena Diversity-Dynamic Global Vegetation Model (JeDi-DGVM): A diverse approach to representing terrestrial biogeography and biogeochemistry based on plant functional trade-offs'. In: *Biogeosciences* 10.6, pp. 4137–4177. DOI: 10.5194/bg-10-4137-2013.

Pelletier, J., A. Paquette, K. Mbindo, N. Zimba, A. Siampale, B. Chendauka, F. Siangulube & J. W. Roberts (2018). 'Carbon sink despite large deforestation in African tropical dry forests (miombo woodlands)'. In: *Environmental Research Letters* 13, p. 094017. DOI: 10.1088/1748-9326/aadc9a.

Penuelas, J., T. Rutishauser & I. Filella (2009). 'Phenology Feedbacks on Climate Change'. In: *Science* 324.5929, pp. 887–888. DOI: 10.1126/science.1173004.

Prather, C. M., S. L. Pelini, A. Laws, E. Rivest, M. Woltz, C. P. Bloch, I. Del Toro, C. Ho, J. Kominoski, T. A. S. Newbold et al. (2012). 'Invertebrates, ecosystem services and climate change'. In: *Biological Reviews* 88.2, pp. 327–348. DOI: 10.1111/brv.12002.

R Core Team (2020). *R: A Language and Environment for Statistical Computing*. R Foundation for Statistical Computing. Vienna, Austria. URL: https://www.R-project.org/.

Reich, P. B., M. B. Walters & D. S. Ellsworth (1992). 'Leaf life-span in relation to leaf, plant, and stand characteristics among diverse ecosystems'. In: 62.3, pp. 365–392. DOI: 10.2307/2937116.

Richardson, A. D., T. F. Keenan, M. Migliavacca, Y. Ryu, O. Sonnentag & M. Toomey (2013). 'Climate change, phenology, and phenological control of vegetation feedbacks to the climate system'. In: *Agricultural and Forest Meteorology* 169, pp. 156–173. DOI: 10.1016/j.agrformet.2012.09.012.

Rousseeuw, P. J. (1987). 'Silhouettes: A graphical aid to the interpretation and validation of cluster analysis'. In: *Journal of Computational and Applied Mathematics* 20, pp. 53–65. DOI: 10.1016/0377-0427(87)90125-7.

Ryan, C. M., M. Williams, J. Grace, E. Woollen & C. E. R. Lehmann (2017). 'Pre-rain green-up is ubiquitous across southern tropical Africa: implications for temporal niche separation and model representation'. In: *New Phytologist* 213.2, pp. 625–633. DOI: 10.1111/nph.14262.

Scheiter, S., L. Langan & S. I. Higgins (2013). 'Next-generation dynamic global vegetation models: Learning from community ecology'. In: *New Phytologist* 198.3, pp. 957–969. DOI: 10.1111/nph.12210.

Sjöström, M., J. Ardö, A. Arneth, N. Boulain, B. Cappelaere, L. Eklundh, A. de Grandcourt, W. L. Kutsch, L. Merbold & Y. Nouvellon (2011). 'Exploring the potential of MODIS EVI for modeling gross primary production across African ecosystems'. In: *Remote Sensing of Environment* 115.4, pp. 1081–1089. DOI: 10.1016/j.rse.2010.12.013.

Smith, B. & J. B. Wilson (1996). 'A consumer's guide to evenness indices'. In: *Oikos* 76, pp. 70–82. DOI: 10.2307/3545749.

Stan, K. & A. Sanchez-Azofeifa (2019). 'Tropical dry forest diversity, climatic response, and resilience in a changing climate'. In: *Forests* 10.5, p. 443. DOI: 10.3390/f10050443.

Stevens, N., C. E. R. Lehmann, B. P. Murphy & G. Durigan (2016). 'Savanna woody encroachment is widespread across three continents'. In: *Global Change Biology* 23.1, pp. 235–244. DOI: 10.1111/gcb.13409.

Stöckli, R., T. Rutishauser, I. Baker, M. A. Liniger & A. S. Denning (2011). 'A global reanalysis of vegetation phenology'. In: *Journal of Geophysical Research* 116.G3. DOI: 10.1029/2010jg001545.

Velasque, M. & K. Del-Claro (2016). 'Host plant phenology may determine the abundance of an ecosystem engineering herbivore in a tropical savanna'. In: *Ecological Entomology* 41.4, pp. 421–430. DOI: 10.1111/een.12317.

White, M. A., K. M. de Beurs, K. Didan, D. W. Inouye, A. D. Richardson, O. P. Jensen, J. O'Keefe, G. Zhang, R. R. Nemani, W. J. D. Van Leeuwen et al. (2009). 'Intercomparison, interpretation, and assessment of spring phenology in North America estimated from remote sensing for 1982-2006'. In: *Global Change Biology* 15.10, pp. 2335–2359. DOI: 10.1111/j.1365-2486.2009.01910.x.

Whitecross, M. A., E. T. F. Witkowski & S. Archibald (2017). 'Savanna tree-grass interactions: A phenological investigation of green-up in relation to water availability over three seasons'. In: *South African Journal of Botany* 108, pp. 29–40. DOI: 10.1016/j.sajb.2016.09.003.

Whitley, R., J. Beringer, L. B. Hutley, G. Abramowitz, M. G. De Kauwe, B. Evans, V. Haverd, L. Li, C. Moore, Y. Ryu et al. (2017). 'Challenges and opportunities in land surface modelling of savanna ecosystems'. In: *Biogeosciences* 14.20, pp. 4711–4732. DOI: 10.5194/bg-14-4711-2017.

Wilsey, B. J., D. R. Chalcraft, C. M. Bowles & M. R. Willig (2005). 'Relationships among indices suggest that richness is an incomplete surrogate for grassland biodiversity'. In: *Ecology* 86.5, pp. 1178–1184. DOI: 10.1890/04-0394.

Xia, J., S. Niu, P. Ciais, I. A. Janssens, J. Chen, C. Ammann, A. Arain, P. D. Blanken, A. Cescatti, D. Bonal et al. (2015). 'Joint control of terrestrial gross primary productivity by plant phenology and physiology'. In: *Proceedings of the National Academy of Sciences* 112.9, pp. 2788–2793. DOI: 10.1073/pnas.1413090112.

Yu, Kailiang & Paolo D'Odorico (2015). 'Hydraulic lift as a determinant of tree–grass coexistence on savannas'. In: 207.4, pp. 1038–1051. DOI: 10.1111/nph.13431.

Zani, D., T. W. Crowther, L. Mo, S. S. Renner & C. M. Zohner (2020). 'Increased growing-season productivity drives earlier autumn leaf senescence in temperate trees'. In: 370.6520, pp. 1066–1071. DOI: 10.1126/science.abd8911.

Zhou, Yong, Benjamin J. Wigley, Madelon F. Case, Corli Coetsee & Ann Carla Staver (2020). 'Rooting depth as a key woody functional trait in savannas'. In: 227.5, pp. 1350–1361. DOI: 10.1111/nph.16613.

Supplementary Material

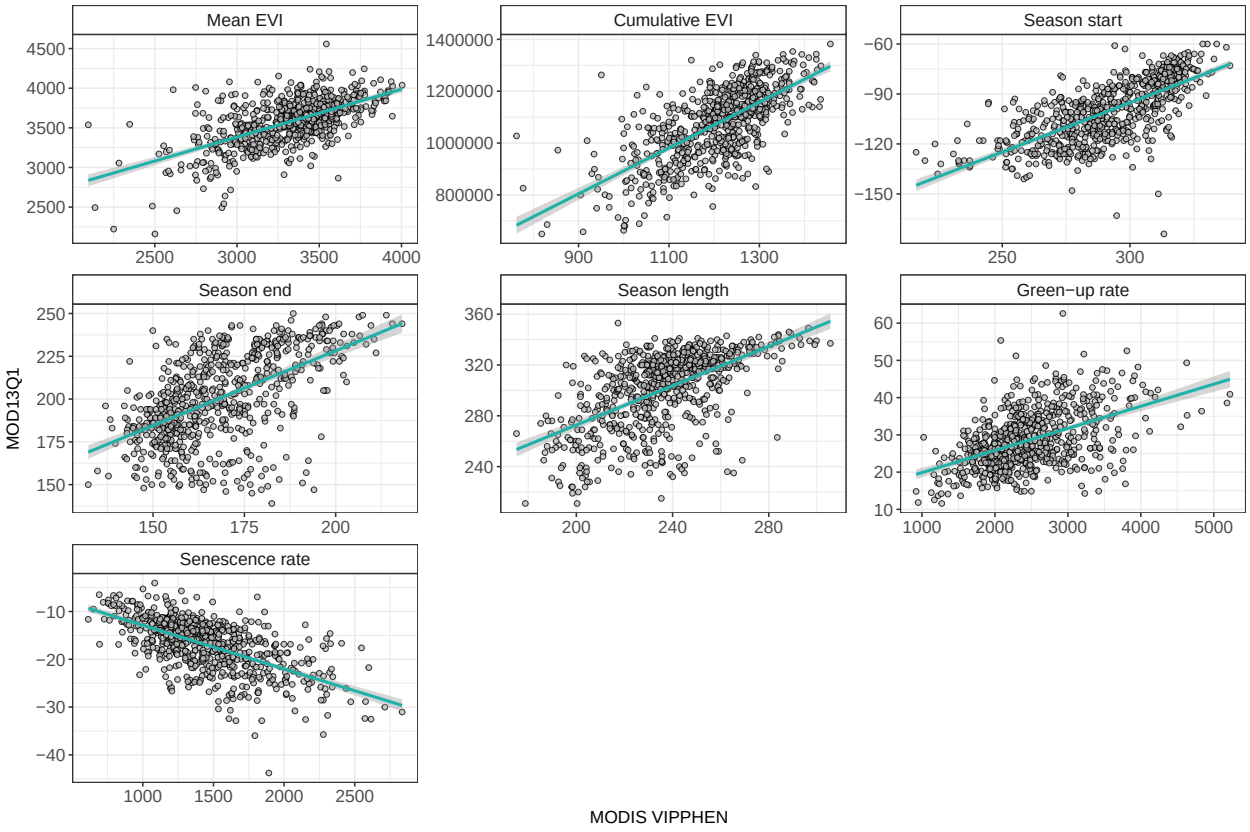

Figure 0.S1: Scatter plots showing a comparison of phenological metrics from the MODIS VIPPHEN product (Didan & Barreto, 2016) and those extracted from the MOD13Q1 data (Didan, 2015), for each of the sites in our study. The cyan line shows a linear model of the data, with a 95% confidence interval.

Response	DoF	F	Prob.	R^2
Mean EVI	672	387.0	$p<0.05$	0.37
Cumulative EVI	672	592.6	$p<0.05$	0.47
Season start	672	660.3	$p<0.05$	0.50
Season end	672	285.0	$p<0.05$	0.30
Season length	672	325.0	$p<0.05$	0.33
Green-up rate	672	217.2	$p<0.05$	0.24
Senescence rate	672	412.3	$p<0.05$	0.38

Table 0.S1: Model fit statistics for comparison of MODIS VIPPHEN and MOD13Q1 products across each of our study sites.

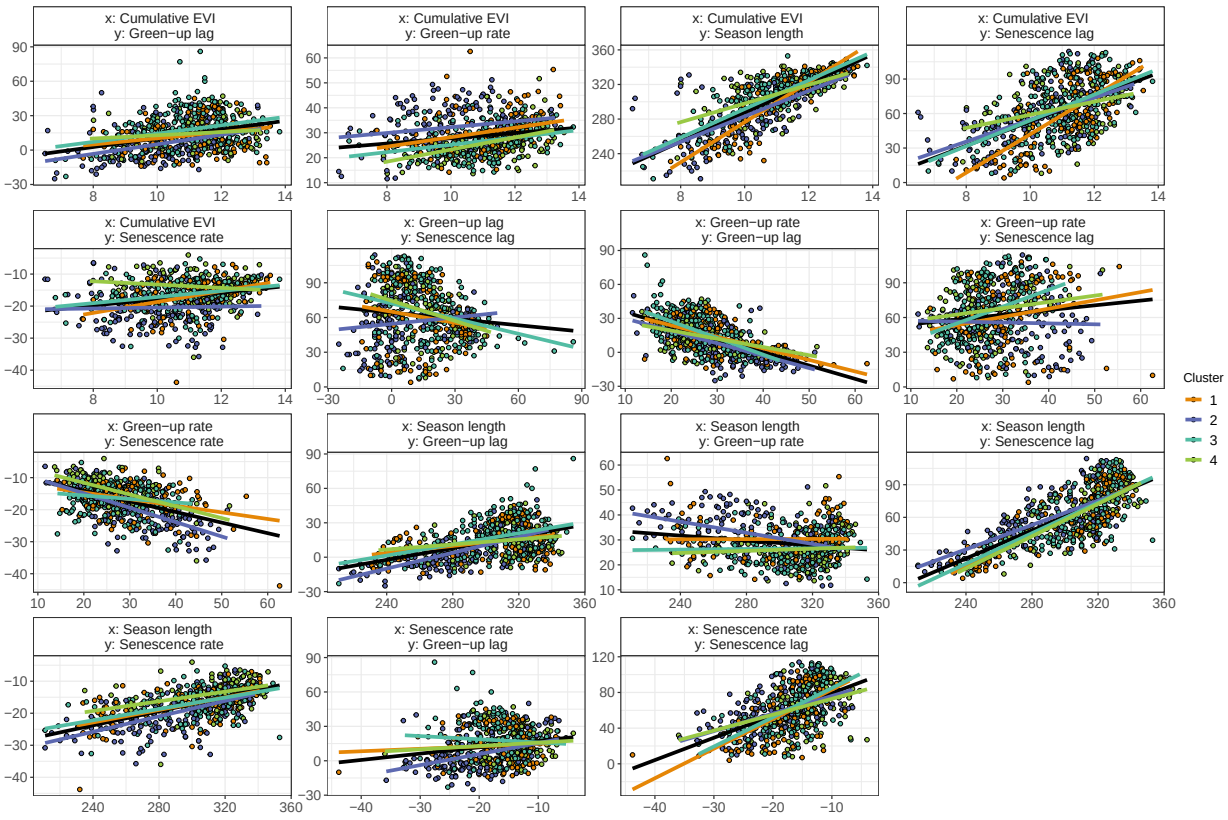

Figure 0.S2: Scatter plots showing pairwise comparisons of the six phenological metrics used in this study, extracted from the MODIS MOD13Q1 product (Didan, 2015). Points represent study sites and are coloured by vegetation cluster. Linear regression line of best fit for all sites is shown as a black line, while linear regressions are shown for each vegetation cluster as coloured lines.

Rank	Precipitation	Stem diameter	Diurnal dT	Richness	Evenness	DoF	logLik	AIC	Δ	W_i
1	✓	✓+	✓	✓+	✓+	**19**	**-932**	**1903**	**0**	**0.380**
2	✓	✓+		✓+	✓+	18	-933	1903	0	0.366
3	✓	✓+	✓	✓	✓+	16	-937	1906	4	0.065
4	✓	✓+		✓	✓+	15	-938	1907	4	0.048
5	✓	✓	✓	✓+	✓+	16	-938	1907	5	0.040
6	✓	✓		✓+	✓+	15	-939	1908	5	0.027
7	✓			✓+	✓+	14	-940	1908	6	0.022
8	✓		✓	✓+	✓+	15	-939	1909	6	0.018
9	✓	✓	✓	✓	✓+	13	-942	1910	8	0.008
10	✓	✓+		✓+	✓	15	-941	1911	9	0.005

Table 0.S2: Cumulative EVI model selection candidate models, with fit statistics. The overall best model is marked by bold text, according to AIC and model parsimony.

Rank	Precipitation	Stem diameter	Diurnal dT	Richness	Evenness	DoF	logLik	AIC	Δ	W_i
1	✓	✓	✓	✓+	✓+	16	-2898	5829	0	0.198
2	✓	✓	✓	✓	✓+	**13**	**-2901**	**5829**	**0**	**0.187**
3	✓	✓		✓+	✓+	15	-2900	5830	1	0.106
4	✓	✓		✓	✓+	12	-2903	5830	1	0.097
5	✓			✓+	✓+	14	-2901	5830	2	0.077
6	✓		✓	✓+	✓+	15	-2900	5831	2	0.074
7	✓			✓	✓+	11	-2904	5831	2	0.068
8	✓		✓	✓	✓+	12	-2903	5831	2	0.064
9	✓	✓+	✓	✓+	✓+	19	-2897	5832	3	0.036
10	✓	✓+	✓	✓	✓+	16	-2900	5832	3	0.034

Table 0.S3: Season length model selection candidate models, with fit statistics. The overall best model is marked by bold text, according to AIC and model parsimony.

Rank	Precipitation	Stem diameter	Diurnal dT	Richness	Evenness	DoF	logLik	AIC	Δ	W_i
1			✓			**6**	**-2071**	**4154**	**0**	**0.165**
2		✓+	✓			10	-2068	4156	2	0.074
3		✓	✓			7	-2071	4156	2	0.074
4			✓	✓		7	-2071	4156	2	0.072
5			✓		✓	7	-2071	4156	2	0.068
6	✓		✓			7	-2071	4156	2	0.067
7	✓	✓+	✓			11	-2068	4157	3	0.038
8		✓+	✓	✓		11	-2068	4157	3	0.036
9		✓	✓	✓		8	-2071	4157	3	0.033
10		✓	✓		✓	8	-2071	4157	3	0.033

Table 0.S4: Green-up rate model selection candidate models, with fit statistics. The overall best model is marked by bold text, according to AIC and model parsimony.

Rank	Precipitation	Stem diameter	Diurnal dT	Richness	Evenness	DoF	logLik	AIC	Δ	W_i
1	✓		✓			7	-1884	3783	0	0.079
2	✓					**6**	**-1886**	**3783**	**1**	**0.059**
3	✓		✓	✓	✓	9	-1883	3784	1	0.055
4			✓			6	-1886	3784	1	0.048
5	✓	✓	✓			8	-1884	3784	1	0.045
6	✓	✓	✓	✓	✓	10	-1882	3784	1	0.044
7	✓		✓	✓		8	-1884	3784	1	0.039
8	✓		✓		✓	8	-1884	3784	2	0.037
9	✓			✓	✓	8	-1884	3785	2	0.034
10	✓				✓	7	-1885	3785	2	0.030

Table 0.S5: Senescence rate model selection candidate models, with fit statistics. The overall best model is marked by bold text, according to AIC and model parsimony.

Rank	Precipitation	Stem diameter	Diurnal dT	Richness	Evenness	DoF	logLik	AIC	Δ	W_i
1	✓		✓	✓	✓	**9**	**-2464**	**4946**	**0**	**0.203**
2	✓		✓	✓+	✓	12	-2461	4946	0	0.190
3	✓	✓	✓	✓+	✓	13	-2460	4947	1	0.119
4	✓	✓	✓	✓	✓	10	-2463	4947	1	0.118
5	✓		✓	✓+	✓+	15	-2458	4947	1	0.109
6	✓		✓	✓	✓+	12	-2461	4947	1	0.105
7	✓	✓	✓	✓	✓+	13	-2461	4948	2	0.061
8	✓	✓	✓	✓+	✓+	16	-2458	4948	2	0.059
9	✓	✓+	✓	✓	✓	13	-2462	4951	5	0.015
10	✓	✓+	✓	✓+	✓	16	-2460	4952	6	0.009

Table 0.S6: Green-up lag model selection candidate models, with fit statistics. The overall best model is marked by bold text, according to AIC and model parsimony.

Rank	Precipitation	Stem diameter	Diurnal dT	Richness	Evenness	DoF	logLik	AIC	Δ	W_i
1	✓	✓	✓	✓+	✓+	16	-2836	5703	0	0.185
2	✓	✓	✓	✓+		**12**	**-2840**	**5704**	**0**	**0.149**
3	✓	✓	✓	✓+	✓	13	-2839	5704	1	0.143
4	✓	✓+	✓	✓+	✓+	19	-2833	5704	1	0.119
5	✓	✓	✓		✓+	12	-2841	5705	2	0.061
6	✓	✓	✓	✓	✓+	13	-2840	5706	2	0.058
7	✓	✓	✓			8	-2845	5706	3	0.038
8	✓	✓+	✓	✓	✓+	16	-2837	5707	4	0.029
9	✓	✓+	✓	✓+	✓	16	-2838	5707	4	0.026
10	✓	✓+	✓		✓+	15	-2839	5707	4	0.025

Table 0.S7: Senescence lag model selection candidate models, with fit statistics. The overall best model is marked by bold text, according to AIC and model parsimony.

Response	Clusters	Estimate	SE	DoF	T ratio	Prob.
Cumulative EVI	1-2	3.1E-01	1.57E-01	600	1.99	p = 0.19
	1-3	-1.4E-01	1.41E-01	600	-0.97	p = 0.77
	1-4	-3.8E-01	1.77E-01	600	-2.14	p = 0.14
	2-3	-4.5E-01	1.24E-01	600	-3.62	p<0.01
	2-4	-6.9E-01	1.68E-01	600	-4.11	p<0.01
	3-4	-2.4E-01	1.54E-01	600	-1.57	p = 0.40
Season length	1-2	1.1E+01	3.76E+00	603	2.89	p<0.05
	1-3	-7.3E+00	3.39E+00	603	-2.14	p = 0.14
	1-4	-1.2E+01	4.06E+00	603	-2.88	p<0.05
	2-3	-1.8E+01	2.98E+00	603	-6.07	p<0.01
	2-4	-2.3E+01	3.90E+00	603	-5.78	p<0.01
	3-4	-4.4E+00	3.54E+00	603	-1.24	p = 0.60
Green-up lag	1-2	6.5E+00	1.70E+00	606	3.80	p<0.01
	1-3	-3.3E+00	1.57E+00	606	-2.08	p = 0.16
	1-4	-1.9E-01	1.94E+00	606	-0.10	p = 1.00
	2-3	-9.7E+00	1.44E+00	606	-6.75	p<0.01
	2-4	-6.7E+00	1.84E+00	606	-3.62	p<0.01
	3-4	3.1E+00	1.69E+00	606	1.83	p = 0.26
Senescence lag	1-2	5.7E+00	3.29E+00	606	1.73	p = 0.31
	1-3	-3.6E+00	2.94E+00	606	-1.22	p = 0.61
	1-4	-5.5E+00	3.64E+00	606	-1.50	p = 0.44
	2-3	-9.3E+00	2.61E+00	606	-3.56	p<0.01
	2-4	-1.1E+01	3.48E+00	606	-3.21	p<0.01
	3-4	-1.9E+00	3.14E+00	606	-0.60	p = 0.93

Table 0.S8: Comparisons of species diversity interaction marginal effects using post-hoc Tukey's tests.

Response	Clusters	Mean diff.	Interval	Prob.
Cumulative EVI	2-1	-0.74	-1.04 - -0.45	p<0.01
	3-1	-0.14	-0.4 - 0.13	p = 0.55
	4-1	0.09	-0.24 - 0.42	p = 0.89
	3-2	0.61	0.35 - 0.87	p<0.01
	4-2	0.84	0.51 - 1.16	p<0.01
	4-3	0.23	-0.07 - 0.53	p = 0.19
Season length	2-1	-0.58	-0.88 - -0.29	p<0.01
	3-1	0.16	-0.1 - 0.43	p = 0.37
	4-1	0.31	-0.01 - 0.64	p = 0.07
	3-2	0.75	0.49 - 1.01	p<0.01
	4-2	0.9	0.58 - 1.22	p<0.01
	4-3	0.15	-0.15 - 0.44	p = 0.56
Green-up rate	2-1	0.26	-0.03 - 0.55	p = 0.11
	3-1	-0.48	-0.74 - -0.22	p<0.01
	4-1	-0.51	-0.84 - -0.19	p<0.01
	3-2	-0.74	-1 - -0.48	p<0.01
	4-2	-0.77	-1.1 - -0.45	p<0.01
	4-3	-0.03	-0.33 - 0.26	p = 0.99
Senescence rate	2-1	-0.65	-0.94 - -0.37	p<0.01
	3-1	0.09	-0.16 - 0.35	p = 0.79
	4-1	0.52	0.2 - 0.84	p<0.01
	3-2	0.75	0.49 - 1	p<0.01
	4-2	1.17	0.86 - 1.49	p<0.01
	4-3	0.43	0.14 - 0.71	p<0.01
Green-up lag	2-1	-0.49	-0.79 - -0.2	p<0.01
	3-1	0.28	0.01 - 0.54	p<0.05
	4-1	0.08	-0.25 - 0.41	p = 0.91
	3-2	0.77	0.51 - 1.03	p<0.01
	4-2	0.58	0.25 - 0.9	p<0.01
	4-3	-0.19	-0.49 - 0.1	p = 0.34
Senescence lag	2-1	-0.19	-0.5 - 0.12	p = 0.38
	3-1	0.15	-0.12 - 0.43	p = 0.47
	4-1	0.22	-0.12 - 0.56	p = 0.36
	3-2	0.34	0.08 - 0.61	p<0.01
	4-2	0.41	0.07 - 0.74	p<0.05
	4-3	0.06	-0.25 - 0.37	p = 0.95

Table 0.S9: Post-hoc Tukey's pairwise comparisons among vegetation types for each phenological metric.